Journal of Rajasthan Academy of Physical Sciences
ISSN : 0972-6306; URL : http://raops.org.in
Vol.14, No.3&4, September-December, 2015, 323-336

ENTROPY ANALYSIS FOR MAGNETOHYRODYNAMIC FLUID FLOW IN POROUS MEDIUM DUE TO A NON ISOTHERMAL STRETCHING SHEET

Paresh Vyas* and Nupur Srivastava**
*Department of Mathematics, University of Rajasthan, Jaipur - 302004
**Department of Mathematics, Poornima University, Jaipur

Abstract: The paper considers the second law analysis of MHD boundary-layer flow heat transfer due to a permeable non isothermal linearly stretching sheet placed at the bottom of fluid saturated porous medium. A uniform suction/blowing is applied. Similarity transformation is performed to convert the governing partial differential equations into ordinary differential equations. The momentum equation has closed form solution which is used in the energy equation. The energy equation is solved numerically by finite difference method. Solutions obtained for velocity and temperature fields are utilized to compute entropy generation. The effects of pertinent parameters on entropy generation are depicted graphically and discussed.

Key Words: Entropy, **s**tretching sheet, inclined magnetic field, suction and blowing.

1. Introduction

Second law of thermodynamics is pivotal for optimal design of thermal systems "aspiring" thermodynamic efficiency. A physical quantity termed "entropy" defined in the second law of thermodynamics is a pertinent measure of irreversibility of real systems. Entropy analysis has emerged as a self sustained research field owing to natural want of optimal thermal systems. Last decade has witnessed a great surge of research activity in entropy generation aspects in convective flow systems. The investigations have been carried out theoretically in idealized flow configurations having technological implications. In fact, in order to find a compromise between hydrodynamic and thermal performance, a second law analysis is a pertinent tool.

There are many causes to entropy production in a fluid flow such as heat transfer, fluid friction, imposed magnetic field, radiative heat transfer, etc. Bejan [7-9] in his pioneer works, has shown that in convective heat transfer processes the parameters which are decisive in entropy generation can be identified and "played with" to optimize the plan for lesser entropy generation. Acknowledging the importance of entropy optimization many authors have reported pertinent relevant studies in diverse convective flow

systems. In view of application of entropy analysis in variety of engineering fields like heat exchangers, cooling of nuclear reactors, energy storage systems, cooling of electronic devises, pumps, turbine, and pipe networks, etc. it has recently become a hot topic of study. It has been studied for variety of fluids in geometries like - channels, tubes and ducts.

The second law analysis to a viscous fluid in a circular duct with isothermal conditions was performed by Sahin [25]. Narusawa [23] gave an analytical and numerical analysis of the second law for flow and heat transfer inside a rectangular duct. Mahmud and Fraser [22] performed thermodynamic analysis of flow and heat transfer inside channel with two parallel plates. Hooman [20] performed entropy analysis in a porous saturated circular tube considering variable viscosity. The effects of magnetic field and viscous dissipation on entropy generation in a falling film and channel were studied by Aïboud-Saouli et al.[1-2]. Chauhan and Olkha [11] studied entropy generation for non-Newtonian fluid flow in a pipe with naturally permeable boundaries. Chauhan and Kumar [12] presented entropy analysis for third-grade fluid flow in annulus partially filled with a porous medium. Vyas and Rai [29] discussed entropy regime for radiative MHD Couette flow inside a channel with naturally permeable base.

The study of boundary - layer flow and/or heat transfer due to a stretching sheet attracted investigators owing to varied applications in engineering and technological processes such as, aerodynamic extrusion of plastic sheets, extrusion of polymers, continuous casting etc. Since the pioneer works of Sakiadis [26] and Crane [15], the fluid flow and heat transfer due to stretching surface have been explored to a vast extent taking into account variety of assumptions and different configurations pertaining to velocity temperature and fluids. Arunachalam and Rajappa [5], Grubka and Bobba [17], Chiam [14], Anderson and Valnes [4], Ali and Yousuf [2], Vyas and Ranjan [27], Vyas and Srivastava [30-31], Vyas and Rai [28], Hayat et al. [18-19], Ibrahim and Shanker [21].

Entropy generation in a fluid flow due to stretching surface in the presence of magnetic field has been analyzed by Aïboud and Saouli [6] and Chauhan and Rastogi [13]. Dehsara et al. [16] discussed entropy analysis for MHD flow over a non-linear inclined transparent plate in a porous medium taking solar radiation into account. Bhutt and Ali [10] showed that magnetic field is a strong source of entropy generation in case of radially stretching sheet. Noghrehabadi et al. [24] presented entropy analysis for Nano fluid flow over a stretching sheet in the presence of heat generation/ absorption and partial slip.

However, a rapid search of the literature reveals that the entropy generation analysis for the set up considered here has not been reported yet though porous medium enjoy advantageous capabilities for heat transfer augmentation.

In view of this, the present paper performs second law analysis of MHD boundary-layer flow due to a permeable non isothermal linearly stretching sheet placed at the bottom of fluid saturated porous medium in the presence of uniform suction/blowing.

1. Mathematical Formulation

A steady two-dimensional boundary layer flow of a viscous, incompressible conducting fluid due to stretching of a heated deformable permeable sheet placed at the bottom of fluid saturated porous medium is considered. Two equal and opposite forces are applied to stretch the sheet, keeping the origin fixed. It is assumed that the speed of a point on the sheet is proportional to its distance from the origin. A Cartesian system of coordinates is used. The x- axis is along the sheet and y-axis is taken normal to it (Figure 1). It is assumed that the wall temperature i.e. the temperature at the sheet $T_w(x) > T_\infty$, where T_∞ is the uniform temperature of the ambient fluid. A constant suction/blowing parallel to y axis is applied at the sheet.

A magnetic field of strength B_0 is imposed inclined at an angle β to the x-axis. The induced magnetic field is neglected, which is valid for small magnetic Reynolds number. Further, we assume that the electric field due to the polarization of charges is negligible. Under these assumptions along with boundary-layer approximations, the system of equations governing the flow in porous medium neglecting the dissipative effects is given as follows,

$$\frac{\partial u}{\partial x}+\frac{\partial v}{\partial y}=0 \tag{1}$$

$$u\frac{\partial u}{\partial x}+v\frac{\partial u}{\partial y}=\vartheta\frac{\partial^2 u}{\partial y^2}-\frac{\vartheta u}{K_0}-\frac{\sigma}{\rho}\left(B_0^2\sin^2\beta\right)u \tag{2}$$

$$u\frac{\partial T}{\partial x}+v\frac{\partial T}{\partial y}=\frac{k}{\rho C_P}\frac{\partial^2 T}{\partial y^2} \tag{3}$$

and the associated boundary conditions are

$$\begin{aligned} &y=0: \quad u=u_w(x)=cx,\ v=v_0,\ T=T_w(x)=T_\infty+Bx^\alpha \\ &y\to\infty: \quad u=0, \quad T=T_\infty \end{aligned} \tag{4}$$

where (u,v) are the velocity components in (x,y) directions, ϑ is the kinematic viscosity of the fluid, σ is the electrical conductivity, μ is the coefficient of viscosity, K_0 is the permeability, ρ is the density, T is the temperature, k is the thermal conductivity, C_P is the specific heat at constant pressure, B, α, $c > 0$ and v_0 are given constants. It must be noted that $v_0 > 0$ corresponds to the case of blowing and $v_0 < 0$ for the case of suction.

2. Solution

The continuity equation (1) is satisfied by introducing a stream function ψ such that

$$u = \frac{\partial \psi}{\partial y}, \quad v = -\frac{\partial \psi}{\partial x} \tag{5}$$

We prescribe the following similarity transformations

$$\eta = \sqrt{\frac{c}{\vartheta}}\, y, \quad \psi = \sqrt{c\vartheta}\, x f(\eta), \quad \theta(\eta) = \frac{T - T_\infty}{T_w - T_\infty} \tag{6}$$

From equations (5)-(6) we obtain

$$u = cx f'(\eta), \quad v = -\sqrt{\vartheta c}\, f(\eta) \tag{7}$$

Following the similarity transformation, the momentum and energy equations (2) – (3) result into following ordinary differential equations respectively.

$$f''' + ff'' - f'^2 - \frac{f'}{K} - M^2 \sin^2\beta\, f' = 0 \tag{8}$$

$$\theta'' + \Pr f\theta' - \Pr \alpha f'\theta = 0 \tag{9}$$

subject to the boundary conditions

$$\begin{aligned} &\eta = 0: \quad f = \lambda, \quad f' = 1, \quad \theta = 1 \\ &\eta \to \infty: \quad f' = 0, \quad \theta = 0 \end{aligned} \tag{10}$$

where prime denotes the differentiation with respect to η. Here K, M, Pr and λ are the permeability parameter, Magnetic field parameter, Prandtl number and blowing (λ<0) / suction (λ>0) parameter respectively defined as

$$K = \frac{cK_0}{\vartheta}, \quad M = \sqrt{\frac{\sigma B_0^2}{c\rho}}, \quad \Pr = \frac{\mu C_P}{k} \quad \text{and} \quad \lambda = \frac{-v_0}{\sqrt{\vartheta c}}$$

The momentum equation (8) in view of end conditions given in equation (10) admits exponential solution of the form

$$f(\eta) = \frac{1}{s}(1 + \lambda s - e^{-s\eta}) \tag{11}$$

where

$$s = \frac{1}{2}\left(\lambda + \sqrt{\lambda^2 + 4(1 + M^2 \sin^2\beta + \frac{1}{K})}\right) \tag{12}$$

The skin friction coefficient in non-dimensional form is given as $\tau = \frac{\tau^*}{\mu c x \sqrt{c/\vartheta}} = f''(0) = -s$ which has been computed numerically.

Using equation (11), the energy equation (9) can be written as

$$\theta'' - \Pr \alpha \theta e^{-s\eta} + \frac{\Pr}{s}(1 + \lambda s - e^{-s\eta})\theta' = 0 \tag{13}$$

The boundary value problem [BVP] given by equation (13) and boundary conditions (10) is highly non-linear and is not amenable to analytic / closed form solution, consequently a numerical solution scheme has been resorted to. The BVP has been solved by finite difference scheme.

3.1 Solution Technique: Finite Difference Method

In order to solve the BVP by finite difference method, discretization of the solution space $[0,\eta_\infty]$ and the derivatives is done which results into a system of algebraic equations. In the present case, the solution space is broken into 'n' equal parts of width '$\Delta\eta$'. Further, the derivatives occurring in the BVP are replaced by appropriate difference approximations at each interior grid point in the solution space. The above system of difference equations at each grid point results into tridiagonal system of linear equations which is solved by Gauss elimination method. The accuracy of the method is ensured by optimal choices of the step size.

After, rigorous grid independence study, it was found that $\Delta\eta = 0.1$ was sufficient to ensure accuracy of 10^{-8} magnitude in all cases. Thus, after computing θ at each grid point we are able to draw profiles for the temperature distributions for varying values of pertinent parameters.

Having determined the velocity and temperature, we embark on to compute entropy generation in the system.

3. Second Law Analysis

The local volumetric rate of entropy generation S_G in the presence of magnetic field is given by (Aïboud and Saouli [6])

$$S_G = \frac{k}{T_\infty^2}\left(\left(\frac{\partial T}{\partial x}\right)^2 + \left(\frac{\partial T}{\partial y}\right)^2\right) + \frac{\mu}{T_\infty}\left(\frac{\partial u}{\partial y}\right)^2 + \frac{\sigma B_0^2 u^2 \sin^2\beta}{T_\infty} + \frac{\mu u^2}{T_\infty K_0} \tag{14}$$

It is clearly visible from the equation (14) that four sources contribute in entropy generation. The first term shows the contribution of heat transfer to entropy across boundary layer, the second term is the local entropy generation due to fluid friction, the third term signifies the effect of magnetic field in the generation of entropy and the last term gives the local entropy generation due to the friction offered by the porous medium.

In order to define the dimensionless entropy generation rate we prescribe the characteristic entropy generation rate S_{G0}, the dimensionless temperature difference Ω and the non-dimensional number for entropy generation N_s respectively as follows

$$S_{G0} = \frac{ck(T_w - T_\infty)^2}{\vartheta T_\infty^2}, \quad \Omega = \frac{T_\infty}{T_w - T_\infty} \quad \text{and} \quad N_s = \frac{S_G}{S_{G0}} \tag{15}$$

Thus the entropy generation number N_s is found to be

$$N_s = \frac{\alpha^2}{X^2}\theta^2 + \theta'^2 + Br\Omega\left(s^2 e^{-2s\eta} + \frac{1}{Ks^2}(1 + se^{-s\eta})^2 + M^2 \sin^2\beta \right) \tag{16}$$
$$= N_1 + N_2$$

where

$$N_1 = \frac{\alpha^2}{X^2}\theta^2 + \theta'^2 \text{ is the Heat transfer irreversibility (HTI),}$$
$$N_2 = Br\Omega\left(s^2 e^{-2s\eta} + \frac{1}{Ks^2}(1 + se^{-s\eta})^2 + M^2 \sin^2\beta \right) \tag{17}$$
$$\text{is the Fluid friction irreversibility (FFI)}$$

$Br = \dfrac{\mu c^2 x^2}{k(T_w - T_\infty)^2}$ stands for Brinkman number and

$X = \dfrac{x}{\sqrt{\vartheta / c}}$ is the dimensionless length along x axis.

The Bejan Number Be which is pertinent irreversibility parameter is defined as follows

$$Be = \frac{HTI}{HTI + FFI} = \frac{N_1}{N_1 + N_2} \tag{18}$$

Here, it should be noted that values 0 and 1 for Be correspond respectively to the cases when the irreversibility is dominated by frictional effects and when the irreversibility due to heat transfer is significant.

4. Results and Discussions

The effects of various parameters on entropy generation number N_s have been shown in figures 2-9 for both the cases - blowing and suction.

The figure 2 indicates that the entropy generation number N_s decreases with an increase in permeability parameter. However, the effect is more pronounced in the case of blowing. This may be attributed to the fact that when blowing takes place then there is

more fluid in the system. Hence, there is much 'activity' in the system in the case of blowing when compared with the counterpart case of suction. That is why entropy is larger in the blowing case as compared to the respective suction case. The figure 3 displays the effect of Hartmann number M and angle of inclination β on the entropy generation number N_s. The very figure reveals that the entropy generation number N_s increases with the increasing values of M and β. In fact, larger values of M and β give rise to larger Joule heating thereby causing loss in energy (exergy destruction). Figure 4 displays the profiles of entropy generation number N_s versus η for varying values of Pr. The figure depicts that N_s decreases with an increase in Pr. This may be attributed to decrease in the temperature gradients with the increasing values of Pr. Figure 5 displays the effects of blowing /suction parameter λ on entropy generation. It is found that with increasing values of blowing parameter ($\lambda<0$), the entropy generation number N_s increases, whereas N_s decreases with the increasing values of suction parameter ($\lambda>0$). Figure 6 displays the effects of wall temperature parameter α on entropy generation. It is found that the entropy generation number N_s increases with the increasing values of α. Figure 7 shows the effect of Brinkman number Br on the entropy generation. It is found that the entropy generation number N_s increases considerably with the increasing values of Brinkman number Br. This goes well with the expectation since larger values of Br are indicative of larger frictional heating in the system.

The figure 8 exhibits the effect of characteristic temperature ratio Ω on entropy generation and shows that the entropy generation number N_s increases with the increasing values of characteristic temperature ratio Ω. Figure 9 depicts the effect of dimensionless length X on entropy generation and shows that entropy generation number N_s decreases as we move away from origin. Thus, the sheet itself serves as a source of irreversibility.

The effects of various parameters on Bejan Number are shown in shown in figures 10-17 for both the cases - blowing and suction.

The figure 10 shows the variation of Bejan number Be with the permeability parameter K. It is clear that Bejan Number Be decays considerably with the increasing values of K. It should be recalled that larger values of K are indicative of easier fluid traversal inside the porous matrix. This gives rise to fluid friction irreversibility due to internal fluid friction and dissipative energy due to resistance offered by the walls of porous matrix. Since Be is the ratio of HTI and (HTI+FFI), hence one can understand the decay in Be for larger values of K. Figure 11 shows that the Bejan number Be decays with the increasing values of M and β in the case of suction. However the trend is not uniform for these variations for blowing case. Figure 12 shows the variation of Bejan number with the Prandtl number and clearly indicates that Bejan number decreases with an increase in Pr. Figure 13 exhibits that with an increase in the blowing/suction parameter λ Bejan number also decreases. Figure 14 shows the variation of Bejan number with the wall temperature parameter α and shows that Bejan number increases with increase in α. Figures 15-17 show the variation of Bejan number Be with the Brinkman number Br, characteristic temperature ratio Ω and dimensionless length X respectively. It is clearly visible from

these figures that Bejan number decreases with an increase in all the three parameters - Br, Ω and X.

Skin friction coefficient measures the viscous drag at the stretching sheet. The effect of various parameters on the skin friction coefficient is shown in figure 18. It is clear from the figure that the skin friction coefficient increases with an increase in the permeability parameter, decrease in the magnetic field parameter M and angle of inclination β. A decrease in the skin friction coefficient is produced with an increase in the suction parameter and reverse trend is observed for decreasing values of the blowing parameter.

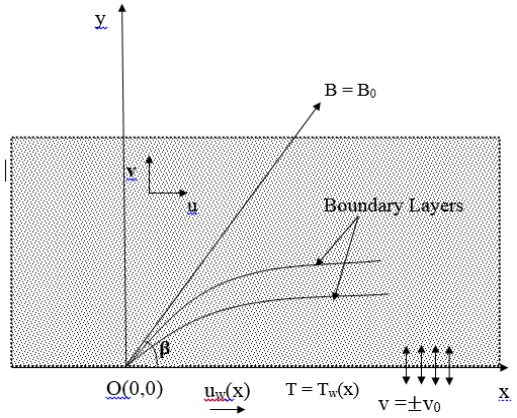

Figure 1: Flow Configuration and Coordinate System

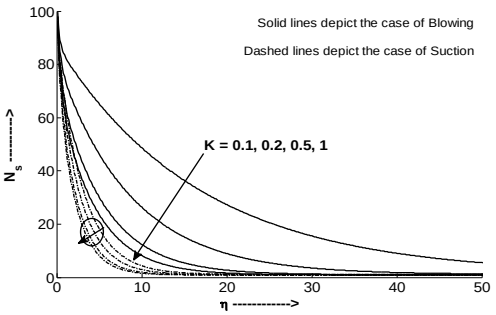

Figure 2: Entropy generation number for variation in K when M = 2, β = π / 4 , α = 2, Pr = 0.71, Br = 2, Ω = 0.2, X = 0.2 and λ = - 0.2 (blowing) / 0.2 (suction)

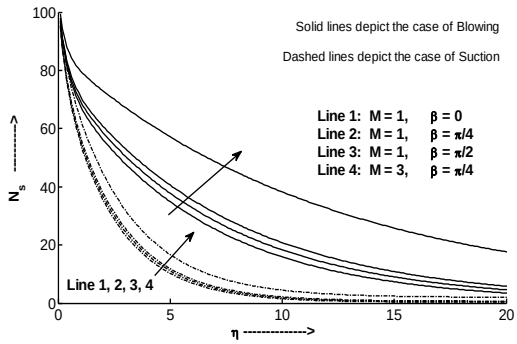

Figure 3: Entropy generation number for variation in M and β when K = 0.2, α = 2, Pr = 0.71, Br = 2, Ω = 0.2, X = 0.2 and λ = - 0.2 (blowing) / 0.2 (suction)

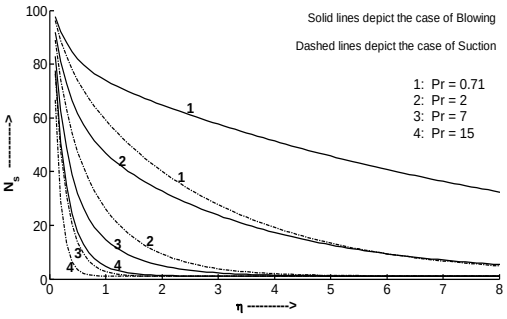

Figure 4: Entropy for variation in Pr when K = 0.2, M = 2, β = π / 4 , α = 2, Br = 2, Ω = 0.2, X = 0.2 and λ = - 0.2 (blowing) / 0.2 (suction)

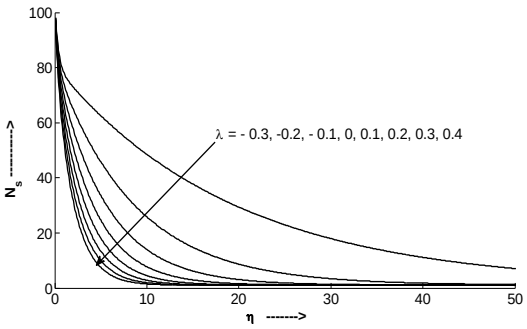

Figure 5: Entropy generation number for variation in λ when K = 0.2, M = 2, β = $\pi / 4$, α = 2, Pr = 0.71, Br = 2, Ω = 0.2 and X = 0.2

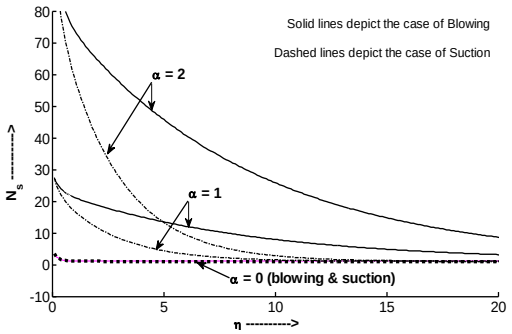

Figure 6: Entropy generation number for variation in α when K = 0.2, M = 2, β = $\pi / 4$, Pr = 0.71, Br = 2, Ω = 0.2, X = 0.2 and λ = - 0.2 (blowing) / 0.2 (suction)

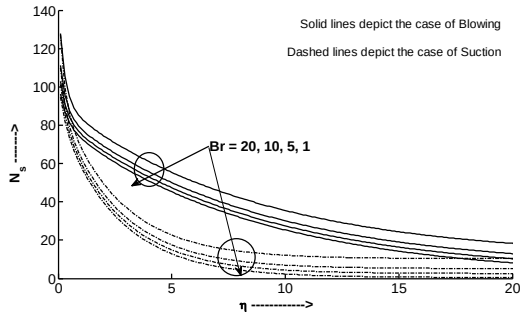

Figure 7: Entropy generation number for variation in Br when K = 0.2, M = 2, β = $\pi / 4$, Pr = 0.71, α = 2, Ω = 0.2, X = 0.2 and λ = - 0.2 (blowing) / 0.2 (suction)

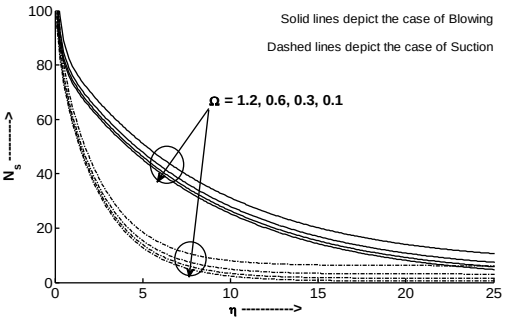

Figure 8: Entropy generation number for variation in Ω when K = 0.2, M = 2, β = $\pi / 4$, Pr = 0.71, α = 2, Br = 0.2, X = 0.2 and λ = - 0.2 (blowing) / 0.2 (suction)

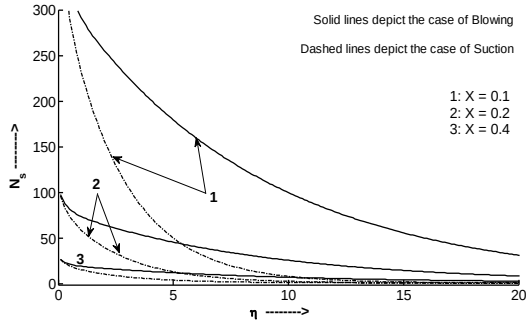

Figure 9: Entropy generation number for variation in X when K = 0.2, M = 2, β = $\pi / 4$, Pr = 0.71, α = 2, Br = 0.2, Ω = 0.2 and λ = - 0.2 (blowing) / 0.2 (suction)

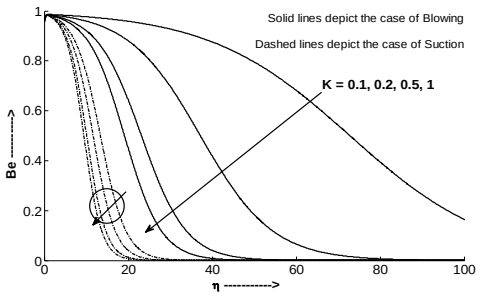

Figure 10: Bejan number for variation in K when M = 2, β = $\pi / 4$, α = 2, Pr = 0.71, Br = 2, Ω = 0.2, X = 0.2 and λ = - 0.2 (blowing) / 0.2 (suction)

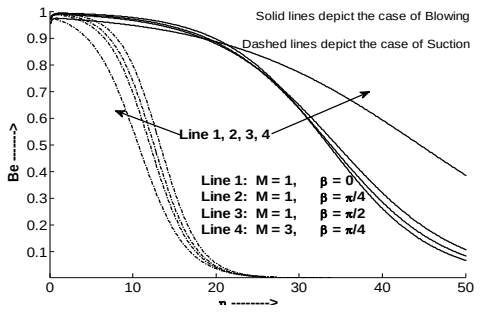

Figure 11: Bejan number for variation in M and β when K = 0.2, α = 2, Pr = 0.71, Br = 2, Ω= 0.2, X = 0.2 and λ = - 0.2 (blowing) / 0.2 (suction)

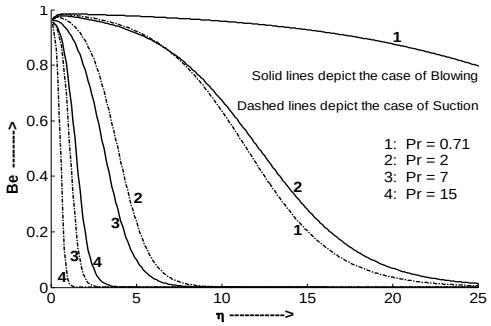

Figure 12: Bejan number for variation in Pr when K = 0.2, M = 2, β = $\pi / 4$, α = 2, Br = 2, Ω = 0.2, X = 0.2 and λ = - 0.2 (blowing) / 0.2 (suction)

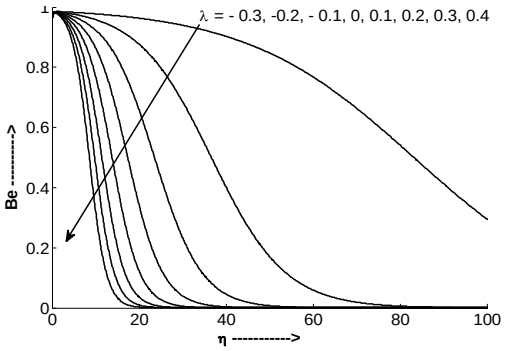

Figure 13: Bejan number for variation in λ when K = 0.2, M = 2, β = $\pi / 4$, α = 2, Pr = 0.71, Br = 2, Ω = 0.2 and X = 0.2

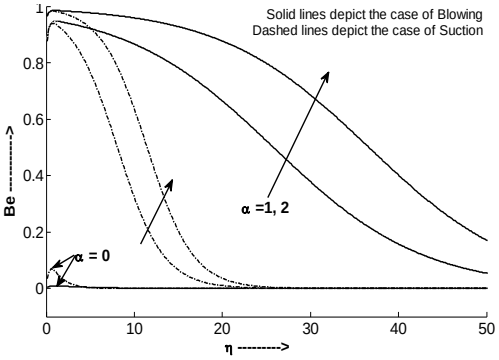

Figure 14: Bejan number for variation in α when K = 0.2, M = 2, β = $\pi / 4$, Pr = 0.71, Br = 2, Ω = 0.2, X = 0.2 and λ = - 0.2 (blowing) / 0.2 (suction)

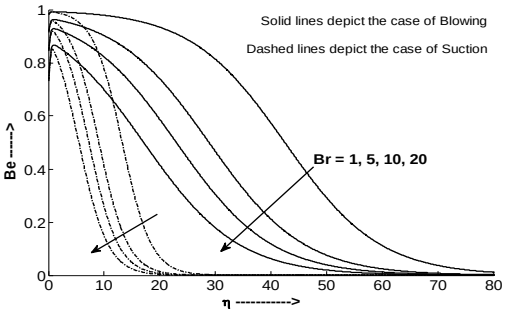

Figure 15: Bejan number for variation in Br when K = 0.2, M = 2, β = $\pi / 4$, Pr = 0.71, α = 2, Ω = 0.2, X = 0.2 and λ = - 0.2 (blowing) / 0.2 (suction)

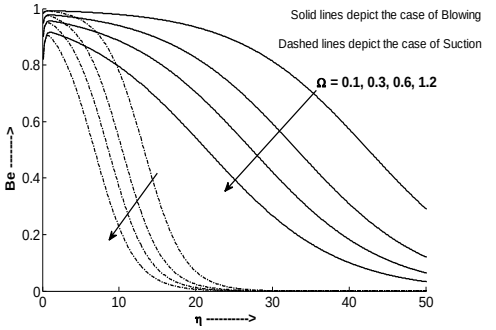

Figure 16: Bejan number for variation in Ω when K = 0.2, M = 2, β = $\pi / 4$, Pr = 0.71, α = 2, Br = 0.2, X = 0.2 and λ = - 0.2 (blowing) / 0.2 (suction 0.2 (suction)

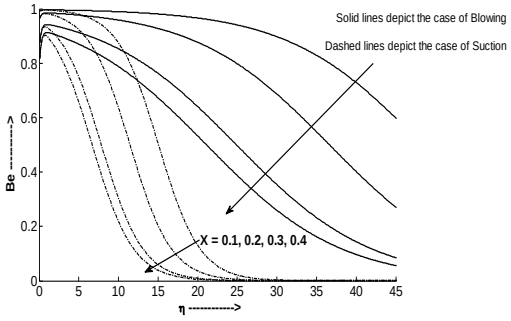

Figure 17: Bejan number for variation in X when K = 0.2, M = 2, $\beta = \pi / 4$, Pr = 0.71, $\alpha = 2$, Br = 0.2, $\Omega = 0.2$ and $\lambda = -0.2$ (blowing) / 0.2 (suction)

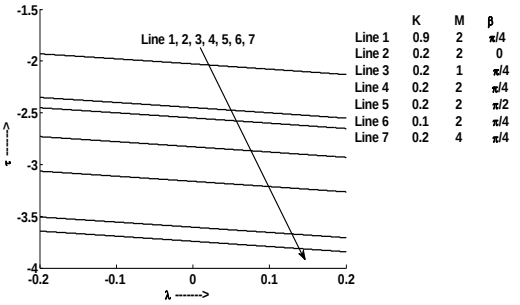

Figure 18: Skin Friction coefficient for variation in K, M and β for both blowing and suction

5. Conclusion

A mathematical simulation has been undertaken for the flow, heat transfer and entropy analysis in a steady flow of a conducting fluid over a non-isothermal linearly stretching sheet in porous medium subject to suction/blowing. The governing boundary layer equations are converted to ordinary differential equations by using similarity transformations. A closed form solution is obtained for the momentum equation which is used in the energy equation. The energy equation is highly non-linear hence has been solved numerically by finite difference scheme. The velocity and temperature fields are utilized to compute entropy generation. We observe that:-

1. Entropy generation number increases with an increase in Hartmann number and its angle of inclination, wall temperature parameter, Brinkman number and characteristic temperature ratio.
2. Entropy generation number deceases with an increase in the permeability parameter, blowing/suction parameter, Prandtl number and non-dimensional length.
3. Bejan number decreases with an increase in permeability parameter, Hartmann number and angle of inclination of imposed magnetic field, Prandtl number, wall temperature parameter, Brinkman number, characteristic temperature ratio and the non-dimensional length.
4. Bejan number increases with an increase in blowing/suction parameter.
5. Skin Friction coefficient increases with an increase in permeability parameter while it decreases with an increase in Hartmann number and its angle of inclination.

Acknowledgement

The authors are thankful to the Referee for valuable comments and suggestions.

References

[1] Aïboud-Saouli, S., Saouli, S., Settou, N. and Meza, N. (2006). Thermodynamic analysis of gravity-driven liquid film along an inclined heated plate with hydromagnetic and viscous dissipation effects, *Entropy*, 8, 188-199.

[2] Aïboud-Saouli, S., Settou, N., Saouli, S. and Meza, N. (2007). Second-law analysis of laminar fluid flow in a heated channel with hydromagnetic and viscous dissipation effects, *Applied Energy*, 84, 279-289.

[3] Ali M.E. and Al-Yousuf F. (2002). Laminar mixed convection boundary layers induced by a linearly stretching permeable surface, *International Journal of Heat and Mass Transfer*, 45, 4241-4250.

[4] Anderson, H.I. and Valnes, O.A. (1998). Flow of a heated ferrofluid over a stretching sheet in the presence of a magnetic dipole, Acta Meccanica, 128, 39-47.

[5] Aurnachalam, M. and Rajappa, N.R. (1978). Forced convection in liquied metals with variable thermal conductivity and capacity, *Acta Mechanica*, 31, 25–31.

[6] Aïboud, S. and Saouli, S. (2010). Entropy Analysis for viscoelastic Magetohydrodynnamic flow over a stretching surface, *International Journal of Non Linear Mechanics*, 45, 482-489.

[7] Bejan, A. (1979). A study of entropy generation in fundamental convective heat transfer, *J. Heat Transfer*, 101, 718-725.

[8] Bejan, A. (1982). Second-law analysis in heat transfer and thermal design, *Adv. Heat Transfer*, 15, 1-58

[9] Bejan, A. (1996). *Entropy generation minimization*, CRC press, Boca Raton, New York.

[10] Bhutt, A.S. and Ali, A. (2013). Effect of magnetic field on Entropy Generation in flow and transfer due to a radially stretching surface, *Chin. Phys. Lett.*, *3*0, (024701)1-5.

[11] Chauhan, D. S. and Olkha, A. (2011). Entropy generation and heat transfer effects on non-Newtonian fluid flow in annular pipe with naturally permeable boundaries, *International Journal of Energy and Technology*, 3(30), 1-9.

[12] Chauhan, D.S. and Kumar, V. (2013). Entropy Analysis for third-grade fluid flow with temperature dependent viscosity in annulus partially filled with a porous medium, *Theoretical and Applied Mechanics*, 40, 441-464.

[13] Chauhan, D.S. and Rastogi, P. (2011). Heat Transfer and entropy generation in MHD flow through a porous medium past a Stretching Sheet, *International Journal of Energy and Technology*, 3, (paper 15) 1-13.

[14] Chiam, T.C. (1982). Micropolar fluid flow over a stretching sheet, *ZAMM*, 62, 565-568.

[15] Crane, L.J. (1970). Flow past a stretching plane, *Z. Angew Math. Phys*., 21, 645-647.

[16] Dehsara, M., MatinHabibi, M. and Dalir, N. (2012). Entropy analysis for MHD flow over a non-linear stretching inclined transparent plate embedded in a porous medium due to solar radiation, *Mechanika*, 18, 524-533.

[17] Grubka, L.G. and Bobba, K.M. (1985). Heat transfer characteristics of a continuous stretching surface with variable temperature, *ASME Journal of Heat Transfer*, 107, 248-250.

[18] Hayat, T., Quasim, M. and Mesloub, S. (2011). MHD flow and heat transfer over a permeable stretching sheet with slip conditions, *Int. J. Num. Methods in fluids*, 66(8), 963-975.

[19] Hayat, T., Imtiaz, M., Alsaedi, A. and Mansoor, R. (2014). MHD flow of nanofluids over an exponentially stretching sheet in a porous medium with convective boundary conditions, *Chinese Physics B*, 23(5), doi: 10.1088/1674-1056/23/5/054701.

[20] Hooman, K. (2006). Entropy-energy analysis of forced convection in a porous-saturated circular tube considering temperature-dependent viscosity effects, *Int. J. of Energy*, 3(4), 436 – 451.

[21] Ibrahim, W. and Shanker, B. (2014). Magnetohydrodynamic Boundary layer flow and heat transfer of a Nanofluid over non-isothermal stretching sheet, *ASME J. of Heat Transfer*, 136(5) 051701(9pages), doi:10.1115/1.4026118.

[22] Mahmud, S. and Fraser, R. A. (2002). Thermodynamic analysis of flow and heat transfer inside channel with two parallel plates, *Exergy*, 2, 140-146.

[23] Narusawa, U. (1998). The second-law analysis of mixed convection in rectangular ducts, *Heat Mass Transfer*, 37, 197-203.

[24] Noghrehabadi, A., Saffarian, M.R., Pourrajab, R. and Ghalambaz, M. (2013). Entropy analysis for nanofluids flow over a stretching sheet in the presence of heat generation/absorption and partial slip, *J. Mech. Sci. Technol.*, 27(3), 927-937.

[25] Sahin, A. Z. (1998). Second law analysis of laminar viscous flow through a duct subjected to constant wall temperature, *J. Heat Transfer,* 120, 76-83.

[26] Sakiadis B.C. (1961). Boundary-layer behaviour on continuous solid surfaces: I. Boundary-layer equations for two dimensional and axisymmetric flow, *AIChE Journal*, 7, 26-28.

[27] Vyas, P. and Ranjan, A. (2010). Dissipative MHD boundary-layer flow in a porous medium over a sheet stretching nonlinearly in the presence of radiation, *Applied Mathematical Sciences*, 4(61-64), 3133–3142.

[28] Vyas, P. and Rai, A. (2012). Radiative MHD dissipative thermal regime in porous medium due to a permeable deforming sheet: Numerical solution, *Modelling, Measurement and Control B*, 81(1-2), 73–86.

[29] Vyas, P. and Rai, A. (2013). Entropy regime for radiative MHD Couette flow inside a channel with naturally permeable base, International J. of Energy & Technology, 5, (paper 19) 1-9.

[30] Vyas, P. and Srivastava, N. (2010). Radiative MHD flow over a non-isothermal stretching sheet in a porous medium, *Applied Mathematical Sciences*, vol. 4(49-52), 2475–2484.

[31] Vyas, P. and Srivastava, N. (2012). On dissipative radiative MHD boundary layer flow in a porous medium over a non-isothermal stretching sheet, Journal of Applied Fluid Mechanics, vol. 5(4), 23–31.